

The optimal Seebeck coefficient for obtaining the maximum power factor in thermoelectrics

P. Pichanusakorn and P. R. Bandaru^{a)}

Department of Mechanical Engineering, Materials Science Program, University of California, San Diego, La Jolla, California 92093-0411, USA

(Received 27 February 2009; accepted 7 May 2009; published online 3 June 2009)

We propose the existence of an optimal Seebeck coefficient (S_{opt}) for three-, two-, and one-dimensional thermoelectric materials. This assertion is supported by an exhaustive comparison with experimental data of well characterized bulk thermoelectrics, all of which have shown that the power factor is maximized when S_{opt} in the range of 130–187 $\mu\text{V}/\text{K}$. Our study serves as a quick guideline for the optimization of thermoelectric materials, and makes the point that efforts should be focused on increasing the electrical conductivity (σ) at the given S_{opt} . © 2009 American Institute of Physics. [DOI: 10.1063/1.3147186]

In order to increase the efficiency of thermoelectric materials, a wide range of bulk^{1,2} and nanostructured^{3,4} materials has been investigated. The extensive scope of this research has led to increased complexity and introduction of many variables such as alloy composition, carrier concentration, temperature, and relevant length scales. Since the thermoelectric figure of merit at a particular temperature T , $ZT = (S^2\sigma/\kappa_e + \kappa_L)T$, is composed of the Seebeck coefficient (S), electrical conductivity (σ), and thermal conductivity from electrons (κ_e) and the lattice (κ_L), each of which responds differently to the variables, the maximization of ZT could be quite a complex task. It would then be necessary and useful to take stock of the situation and identify optimization criteria. In this paper, we present the conditions under which the power factor ($S^2\sigma$) is maximized in *any material, at any temperature* and for *any given electron gas dimensionality* using the reduced Fermi potential, $\eta(=E_F - E_o/k_B T)$, as the dependent variable. The η is correlated with the carrier concentration, n , determined by both the E_F (Fermi energy), measured from a ground state energy level E_o , and the T . Such a criterion allows us to establish the *universal* and *optimal Seebeck coefficient* where power factor is maximized. Our conclusions are valid for systems that can be described by the Boltzmann transport equation (BTE), assuming (a) parabolic band structure, (b) single band/subband approximation, and (c) power-law relaxation time of the form $\tau(E) = \tau_o E^r$, where r and τ_o are the scattering constants.⁵ Such assumptions are satisfied in most materials, and any slight deviations will not affect the results presented here much.

In most materials, the σ and the S are manifestation of carrier (i.e., electrons/holes) diffusion along a concentration gradient, which is established by a gradient of the E_F or T , (we neglect other possible contributions, e.g., phonon drag.⁶) The transport coefficients are given by the steady-state solution to the BTE as¹

$$S = \mp \frac{k_B}{e} \left[\frac{\left(r + \frac{D}{2} + 1\right) F_{r+(D/2)}(\eta)}{\left(r + \frac{D}{2}\right) F_{r+(D/2)-1}(\eta)} - \eta \right], \quad (1)$$

^{a)}Electronic mail: pbandaru@ucsd.edu.

$$\sigma = ne\mu, \quad (2)$$

where the carrier concentration (n) and the electron mobility (μ) are

$$n = \frac{N}{g_D a^{3-D}} \left(\frac{2k_B T m_d}{\hbar^2} \right)^{D/2} F_{(D/2)-1}(\eta), \quad \text{where } g_D = 2\pi^2 \text{ (for } D=3); \quad D\pi \text{ (for } D=2,1), \quad (3)$$

$$\mu = \frac{e \left(\frac{2r}{D} + 1 \right)}{m_\sigma} \tau_o (k_B T)^r \left[\frac{F_{r+(D/2)-1}(\eta)}{F_{(D/2)-1}(\eta)} \right]. \quad (4)$$

Here, $F_j(\eta) = \int_0^\infty [x^j / \exp(x - \eta) + 1] dx$ is the j th order Fermi integral and is evaluated numerically.⁷ N , m_d , and m_σ refer to number of conduction valleys, density of states (DOS) effective mass, and conductivity effective mass, intrinsic to the material. D and a are the electron gas dimensionality factor ($D=3, 2, 1$ for bulk material, quantum well, and nanowire) and relevant length scale (e.g., quantum well/nanowire thickness) pertinent to the device under consideration, respectively. k_B and \hbar are the Boltzmann and the reduced Planck constants, while e is the unit of elementary charge.

The variation of S and σ with η is represented through Figs. 1(a)–1(c). From Eq. (1), S as a function of η is independent of intrinsic material parameters and temperature, and Fig. 1(a) is universal for a given D and r . Since the Seebeck voltage is proportional to the difference of the average electron energy and the lowest energy level (e.g., E_F at 0 K), $|S|$ always increases as η is decreased, i.e., if either T is increased or E_F is decreased. Similarly, while both n and μ , from Eqs. (3) and (4), are dependent on material parameters and temperature, their normalized forms, \tilde{n} in Fig. 1(b) and $\tilde{\mu}$ in Fig. 1(c), are universally applicable to any material at any temperature. In most instances, σ tends to increase with increased E_F (i.e., increased η and n) and/or increased T (i.e., $n \propto T^{D/2}$). Consequently, when n and σ are increased by doping or biasing, which increases E_F and η , $|S|$ is decreased. Consolidating the above results, the power factor ($S^2\sigma$) is seen to always increase with increasing T assuming a constant E_F but exhibits a peak at an optimal E_F when constant T is assumed. Now, considering that (i) $S^2\tilde{n}\tilde{\mu}$ will be maximized at a unique optimal value of reduced Fermi potential

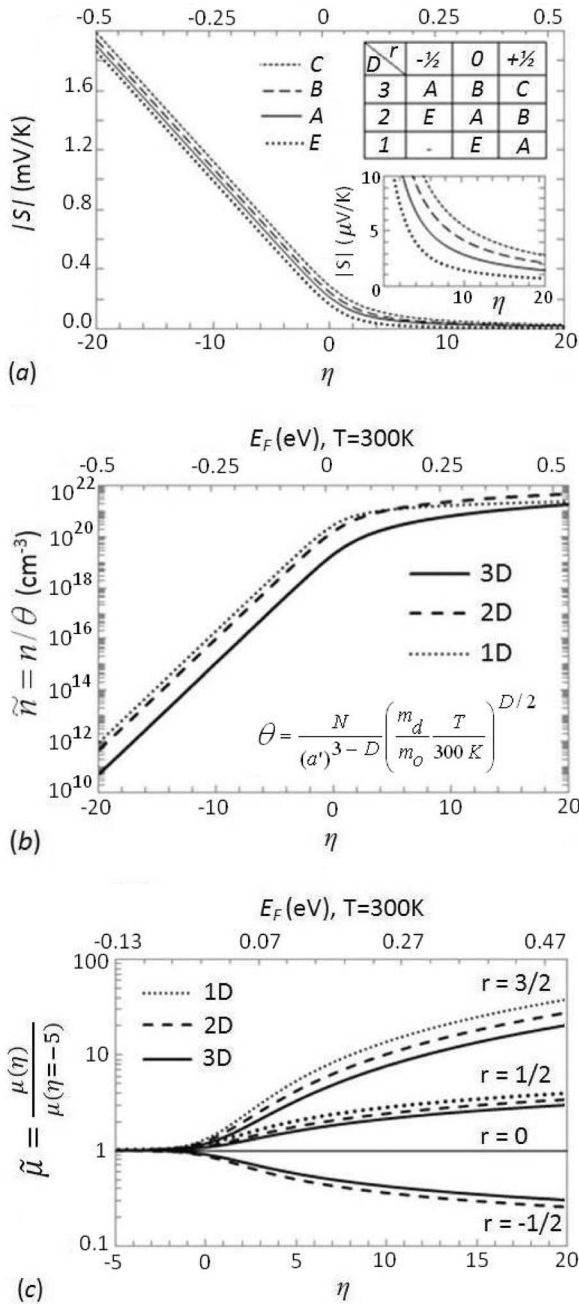


FIG. 1. The variation of (a) the Seebeck coefficient, $|S|$, (b) normalized carrier concentration, \tilde{n} and (c) normalized mobility, $\tilde{\mu}$, as a function of the reduced Fermi potential, η . The equivalent E_F at 300 K is labeled on the top horizontal axis. In the inset table to (a), the $|S|$ is similar for several combinations of r and D . In the inset to (b), the carrier concentration normalization constant, θ , is defined. a' is the width (in nm) of quantum well or nanowire.

(η_{opt}) for a given r and D , but is independent of material and temperature, and that (ii) $S^2\sigma$ is proportional to $S^2\tilde{n}\tilde{\mu}$, it must then be true that the maximum $S^2\sigma$ for any material at any given temperature always occurs at η_{opt} . Consequently, there exists a universal and optimal value of Seebeck coefficient (S_{opt}), which corresponds to η_{opt} through Eq. (1). The optimal carrier concentration could be calculated from Eq. (3), but this value will not be universal, and will vary according to the material and temperature.

By plotting $S^2\tilde{n}\tilde{\mu}$ as a function of η , the η_{opt} has been identified for several values of D and r , as listed in Table I. While η_{opt} generally increases as r or D is increased, when

TABLE I. The value of η_{opt} (top line) and S_{opt} (μ V/K, bottom line) for maximum power factor ($S^2\sigma$) as a function of the scattering constant (r) and dimensionality (D). S is indeterminate for $D=1$ and $r=-1/2$. For $r=+3/2$ ($D=3, 2, 1$) and $r=+1/2$ ($D=3$), the $S^2\sigma$ increases without limit as η is increased. The r changes with D for acoustic and optical phonon deformation potential scattering (i.e., ADP and ODP) and strongly screened ionized impurity scattering, as indicated through grouping, as the scattering rate for these processes is proportional to the DOS.

D	$r = -1/2$	0	$+1/2$	$+3/2$
3	0.67 167	2.47 130	no limit -	no limit -
2	-0.37 187	0.67 167	2.47 130	no limit -
1	n/a -	-0.37 187	0.67 167	no limit -
		Neutral Impurity	ADP ODP	Ionized Impurity (weakly screened)
		Ionized Impurity (strongly screened)		

$r > 0$, i.e., when weakly screened ionized impurity scattering is dominant, the $S^2\sigma$ may increase without limit due to combined increase in n and μ being larger than the reduction in S^2 as η is increased. However, this is not observed in practice as strongly screened scattering, with $r < 0$, dominates at high value of η and n . When multiple scattering processes are concurrent, r may take intermediate values to those listed in Table I. As the Fermi integral changes gradually with incremental changes in its indices (i.e., r), the value of η_{opt} will also change gradually and should follow the trend set forth in Table I. Our results now show that for any material, the maximum $S^2\sigma$ at a given temperature is expected when the $|S|$ is in the range of 130–187 μ V/K.

Literature surveys confirm our expectation of maximum $S^2\sigma$ when $|S|$ approaches S_{opt} , in cases where there is sufficient data. An example is shown for a number of p - and n - Bi_2Te_3 and n - PbTe alloys with various dopant concentrations in Fig. 2. In the range of 75–150 K for Bi_2Te_3 and at

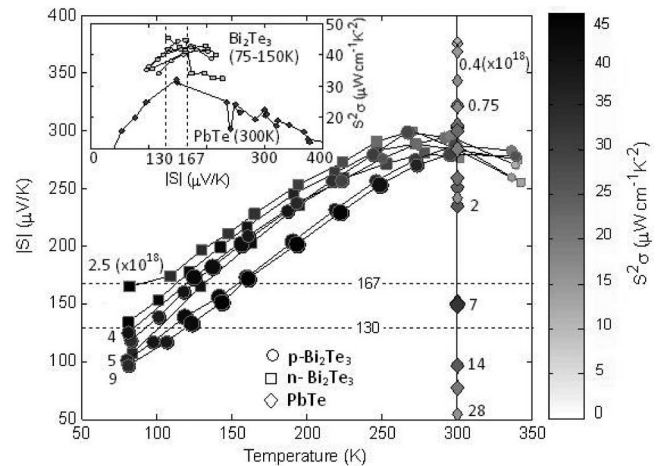


FIG. 2. The variation of $|S|$ and power factor ($S^2\sigma$), with temperature (T), for bulk p - and n - Bi_2Te_3 (see Ref. 8) and n - PbTe (see Ref. 9). The magnitude of $S^2\sigma$ is indicated by the size and shading of each data point, i.e., a larger size and darker shade indicates larger $S^2\sigma$. The carrier concentrations are indicated in units of 10^{18} cm^{-3} . The solid lines serve as a guide for the eye, and connect data of one sample over range of temperature (Bi_2Te_3 based samples) or of different samples at a particular temperature (PbTe). The inset indicates the maximization of $S^2\sigma$ at values close to S_{opt} .

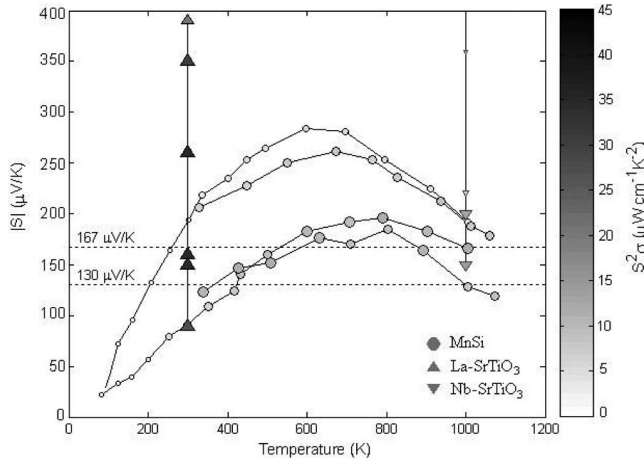


FIG. 3. The variation of $|S|$ and $S^2\sigma$ with T for bulk p -type MnSi (see Ref. 11) and n -type La doped SrTiO₃ (see Ref. 13) and Nb doped SrTiO₃ (see Ref. 12). The maxima in the curves for MnSi are due to the onset of bipolar conduction.

300 K for PbTe, respectively, it is clear that the $S^2\sigma$ is maximized for samples doped such that $|S|$ is close to 130–167 $\mu\text{V}/\text{K}$. For Bi₂Te₃, at $T > 150$ K, it is evident that $S^2\sigma$ increases as $|S|$ decreases toward S_{opt} , and our results predict an *even higher* $S^2\sigma$ as the dopant concentration is increased until $|S| \sim S_{\text{opt}}$. At $T > 250$ K, the onset of bipolar conduction leads to a reduction of both $|S|$ and $S^2\sigma$ for the Bi₂Te₃ alloys.

At high temperature, the intrinsic carrier concentration may be comparable to the dopant concentration, and significant electrical conduction could occur by both electrons and holes. Since the S for the electrons (/holes) is negative (/positive), the average $|S|$ is decreased, which then limits the power factor. The onset temperature of bipolar conduction is lower for materials with a smaller band gap, but increases slightly for samples with larger dopant concentration and lower $|S|$ as observed in Fig. 2. Since bipolar conduction violates our single band assumption, its onset temperature is considered the upper limit for our model. Incidentally, the maximum $S^2\sigma$ in a particular material would be achieved just below this onset temperature, and when $\eta = \eta_{\text{opt}}$.

Our ideas are also applicable to other materials such as SiGe,¹⁰ manganese silicide¹¹ and metal oxides,^{12,13} e.g., SrTiO₃. Similar analysis of p -Si_{0.7}Ge_{0.3} data in the 400–600 K range shows maximization of $S^2\sigma$ as $|S|$ approaches S_{opt} (~ 167 $\mu\text{V}/\text{K}$), while n -Si_{0.7}Ge_{0.3} also shows increasing $S^2\sigma$ as $|S|$ is reduced toward S_{opt} . In Fig. 3, the maximum $S^2\sigma$ of the silicides also occurs at $S_{\text{opt}} \sim 167$ $\mu\text{V}/\text{K}$, with bipolar conduction above 600 K, while both La- and Nb-doped SrTiO₃ also exhibit a maximum $S^2\sigma$ near $S_{\text{opt}} \sim 167$ $\mu\text{V}/\text{K}$, at 300 K (Ref. 13) and 1000 K,¹² respectively.

Currently, the highest $S^2\sigma$ achieved in bulk materials, as seen from Figs. 2 and 3, is approximately 40–45 $\mu\text{W}/\text{cm}^2\text{K}^2$. Such values are consistent with the fact that these materials have similar values of ZT (in the range of 0.8–1) and κ (~ 1 –4 W/mK).¹⁴ As $|S|$ should be close to $S_{\text{opt}} \sim 167$ $\mu\text{V}/\text{K}$, we estimate an $\sigma \sim 1800$ $\Omega^{-1}\text{cm}^{-1}$ for these materials when optimized for maximum $S^2\sigma$. However,

while the $|S|$ and σ are similar, the constituent n and μ can vary significantly. For example, Bi₂Te₃ and PbTe possess small n and large μ due to their small carrier masses, while Si_{1-x}Ge_x and SrTiO₃ have large n and small μ due to large carrier mass. Larger power factors exceeding 100 $\mu\text{W}/\text{cm}^2\text{K}^2$ have been reported in PbTe quantum well^{9,15} and Si/Ge superlattices,^{4,16} where the enhancement has been ascribed to the increased DOS due to electron confinement.⁴ Our predictions of η_{opt} and S_{opt} should also hold for nanostructures and other modified¹⁷ materials to which a BTE based approach may be applicable, although we were unable to find sufficient experimental data on the variation of n (and E_F) in these structures.

In conclusion, we have demonstrated, the existence of a universal optimal reduced Fermi potential (η_{opt}) and the corresponding optimal Seebeck coefficient (S_{opt}), in the range of 130–187 $\mu\text{V}/\text{K}$, where the power factor is maximized at any given temperature. Our findings might help to dispel the notion that good thermoelectrics should have very large $|S|$. Instead, it would help to refocus efforts on increasing the $S^2\sigma$ through an increase in the σ while maintaining $|S| \sim S_{\text{opt}}$. Additionally, the identification of η_{opt} will enable easy determination of the optimal carrier concentration, along with minimum quantum well/nanowire thickness required for an enhancement of the power factor over the bulk values.

We gratefully acknowledge support from the National Science Foundation (Grant No. ECS-05-08514) and the Office of Naval Research (Grant No. N00014-06-1-0234).

- ¹G. S. Nolas, J. Sharp, and H. J. Goldsmid, *Thermoelectrics—Basic Principles and New Materials Development* (Springer, New York, 2001).
- ²G. D. Mahan, *Solid State Physics* (Academic, New York, 1997), Vol. 51, pp. 82–157.
- ³L. D. Hicks and M. S. Dresselhaus, *Phys. Rev. B* **47**, 16631 (1993).
- ⁴L. D. Hicks and M. S. Dresselhaus, *Phys. Rev. B* **47**, 12727 (1993).
- ⁵M. Lundstrom, *Fundamentals of Carrier Transport*, 2nd ed. (Cambridge University Press, Cambridge, 2000).
- ⁶A. I. Boukai, Y. Bunimovich, J. Tahir-Kheli, J.-K. Yu, W. A. Goddard III, and J. R. Heath, *Nature (London)* **451**, 168 (2008).
- ⁷N. Mohankumar and A. Natarajan, *Phys. Status Solidi B* **188**, 635 (1995).
- ⁸V. A. Kutasov, L. N. Lukyanova, and M. V. Vedernikov, in *Thermoelectrics Handbook: Macro to Nano*, edited by D. M. Rowe (CRC, Boca Raton, FL, 2006), p. 37-7.
- ⁹T. C. Harman, D. L. Spears, and M. J. Manfra, *J. Electron. Mater.* **25**, 1121 (1996).
- ¹⁰J. P. Dismukes, L. Ekstrom, E. F. Steigmeier, I. Kudman, and D. S. Beers, *J. Appl. Phys.* **35**, 2899 (1964).
- ¹¹M. I. Fedorov and V. K. Zaitsev, in *Thermoelectrics Handbook: Macro to Nano*, edited by D. M. Rowe, (CRC, Boca Raton, FL, 2006), p. 31-1.
- ¹²T. Okuda, K. Nakanishi, S. Miyasaka, and Y. Tokura, *Phys. Rev. B* **63**, 113104 (2001).
- ¹³S. Ohta, T. Nomura, H. Ohta, M. Hirano, H. Hosono, and K. Koumoto, *Appl. Phys. Lett.* **87**, 092108 (2005).
- ¹⁴G. D. Mahan, *Solid State Physics* (Academic, New York, 1997), Vol. 51, pp. 82–157.
- ¹⁵L. D. Hicks, T. C. Harman, X. Sun, and M. S. Dresselhaus, *Phys. Rev. B* **53**, R10493 (1996).
- ¹⁶R. Venkatasubramanian, E. Siivola, and T. Colpitts, in Proceedings of the 17th International Conference on Thermoelectrics, Nagoya, Japan (IEEE, 1998), pp. 191–197.
- ¹⁷J. P. Heremans, V. Jovic, E. S. Toberer, A. Saramat, K. Kurosaki, A. Charoenphakdee, S. Yamanaka, and G. J. Snyder, *Science* **321**, 554 (2008).